Jordan Journal of Civil Engineering, Volume **14**, No. **1**, **2020**

Reliability Analysis of Rock Slope Using Soft Computing Techniques

Prithvendra Singh [1)*]***, Deepak Kumar*** [2)] ***and Pijush Samui*** [3)]

[1)] National Institute of Technology Patna, Bihar, India. * Corresponding Author.
E-Mail: prithvendra.ce17@nitp.ac.in
[2)] National Institute of Technology Patna, Bihar, India.
E-Mail: decage007@gmail.com
[3)] Associate Professor, Department of Civil Engineering, National Institute of Technology Patna, Bihar, India. E-Mail: pijush@nitp.ac.in

ABSTRACT

Probability of safety (reliability) analysis is a major concern of any structure, especially of rock mechanics. This paper used different machine learning (ML) techniques (cubist model, extreme learning machine (ELM) and multivariate adaptive regression splines (MARS)) for reliability analysis of rock slopes. The performance of these ML models was assessed using different statistical parameters, such as Nash-Sutcliff coefficient (NS), coefficient of determination (R^2), root mean square error (RMSE), variance account factor (VAF), expanded uncertainty (U95), mean absolute error (MAE), … etc. A comparative study was performed to test the adaptability of cubist, ELM and MARS models. It is evident from the results that MARS model shows excellent results in terms of fitness parameters. This study reflects that cubist, ELM and MARS models are well capable of predicting the reliability of slope in terms of the factor of safety (FOS) of rock slope considering statistical predictands.

KEYWORDS: Reliability analysis, Rock slope, Cubist model, ELM, MARS.

INTRODUCTION

Human intervention in the form of construction is increasing significantly over the elapse of time. Random change in climate (i.e., continuous increase in temperature) favours the occurrence of natural disasters in the form of landslide (Liu and Chen, 2007; Zhou et al., 2010). Soil slope failure cannot be determined using slip surface; whereas rock slopes fail generally by slipping along the surface which is structurally weak (Khalokakaie and Zare Naghadehi, 2012; Pariseau, Puri and Schmelter, 2008; Youssef, Pradhan and Al-Harthi, 2015).

Rock slope failure is primarily controlled by weak surfaces, which depends upon two factors: the enhancement of hydrostatic pressure as a result of seepage flow and the reduction in shear strength of the weak surface. These two factors disturb the force balance of the rock slope (Park, West and Woo, 2005; Tan et al., 2013; Topal, 2007). In the case of disturbance and uncontrolled situation, rock slope failure occurs. Further study on failure of rocks has been carried out (Li et al., 2015). In past decades, study of rock slopes (reliability analysis) mainly concentrated on homogeneous slopes. Many assessment methods for homogeneous slopes were proposed (Jimenez-Rodriguez and Sitar, 2007; Wang et al., 2013; Wei et al., 2014). Most of these methods concentrated on Rosenbleuth method, Monte Carlo method and first-order second- moment (FOSM) method (Duzgun, Yucemen and Karpuz, 2003; Ganji and Jowkarshorijeh, 2012; Ge, Tu and Qin, 2011). In

Received on 15/1/2019.
Accepted for Publication on 5/2/2020.

Rosenbleuth method, yielding of stability of slope using reliability index has been done using specific samples at points with stipulated rules (Park, Um et al., 2012; Sun, Zeng and Ding, 2008). Few researchers used Gauss process-based approach for landslide displacement and analysis (Liu, Xu and Shao 2012). While using FOSM method in the calculation of reliability index, partial derivative of the performance function is required (Liang and Xue-Song, 2012).

The relationship between hydrostatics and shear strength plays a vital role in slope reliability (Kourosh, Mosrafa and Heydari, 2011; Li, Zhao and Ru, 2013). There are various deterministic methods, like finite element method, limit equilibrium method, finite difference method and discrete element method, which are available to study rock slope stability (Reale et al., 2015). The above methods of rock slope characterization can only be used to determine safety factor, deformation distribution characteristics and stress (Li, Wang and Cao, 2014; Park, Um et al., 2012; Park et al., 2005). These deterministic methods have limitations, as these methods do not account for the degree of uncertainty during the rock slope stability characterization process (Yang, Zhi-gang, Tong-chun Li and Miao-lin Dai, 2009) and the calculated factor of safety is not suitable for the characterization of stability of the slope as index (Jiang et al., 2014; Li, Tang and Phoon, 2015). Considering the above limitations, several researchers have shifted their focus towards the probabilistic theory to analyze the slope stability problem and calculate the safety factor for rock slope (Gravanis, Pantelidis and Griffiths, 2014; Park et al., 2016; Pathak and Nilsen, 2004). Reviewing recent literature on artificial intelligence (AI) and its applications in various fields of civil engineering motivated the authors to adopt different machine learning techniques (Baecher and Christian, 2003; Duzgun et al., 2003; Ganji and Jowkarshorijeh, 2012; Ge et al., 2011; Harr, 1987; Liang and Xue-song, 2012). In this research, a relatively new machine learning technique called cubist model has been used to analyze rock stability. In addition, a comparative study has been carried out using two other machine learning models (ELM and MARS).

Safety factor (F_s) of slopes having plane failure in rocks has been determined using equations of force balance, using Mohr- Coulomb criteria (Zhou et al., 2017) as in Equation (1).

$$F_s = \frac{cA_2 + \left(Wcos\beta + A_1\sigma_1 cos\alpha\right) tan\varnothing}{Wsin\beta - A_1\sigma_1 sin\alpha} \quad (1)$$

where W, α, β, φ and c are the mass of sliding block, intersection angle of slip surface B with horizontal plane, intersection angle of slip surfaces B and A, internal friction angle and cohesion of slipping surface, respectively. A_1 is the area of rear edge slip surface A and A_2 is the area of bottom slip surface B. The total mass weight has been obtained through geometric analyses and mechanical calculation as 17,420 kN/m, A_1 is 35 m, A_2 is 50 m, α is 40° and β is 32° as from the work of Zhou et al. (2017).

After calculating the factor of safety, performance function (PF) has been obtained using Equation (2).

$$PF = F_s - 1 \quad (2)$$

Performance function (PF) follows normal distribution and the values of PF and β (reliability index) can be calculated using Equation (3).

$$\beta = \frac{\mu(PF)}{\sigma(PF)} \quad (3)$$

where μ(PG) is the mean and σ(PG) is the standard deviation of the performance function PF.

THEORETICAL BACKGROUND OF MODEL USED

CUBIST

Cubist, generally a rule-based model, is an extension of Quinlan's M5 model tree (Quinlan, 2014). Cubist uses the method of recursive partitioning. It splits training cases just like growing a decision tree. It is based on the minimization of intra subset alteration of class value in spite of maximization. Similar to regression trees (Breiman, 2017), it also uses the same divide and conquer rule.

Suppose that we have to construct a model tree for set M of training cases. Now set M will be split according to the outcome of the test. Suppose that M_i represents the subset of *i* outcomes and sd (M_i) is the standard deviation; then, the expected reduction in the value of error can be obtained by using Equation (4).

$$\Delta\ error = sd(M) - \sum \frac{|Mi|}{|M|} \times sd(M_i) \quad (4)$$

As the test proceeds, the model picks the outcome having maximum reduction in the value of error. Cubist model also uses committees, where iterative model trees are created in sequence, which have boosting-like schemes. As the initial tree grows, alteration in the final cubist model occurs by estimation of error through the processes of linear modelling, linear model simplification, pruning and smoothing. Interested readers can find more details on CUBIST in Kuhn et al. (2016).

Extreme Learning Machine (ELM)

Huang (2003) proposed extreme learning machine (ELM) for extensive single hidden layer feedforward neural networks (SLFNs). ELM has gathered more focus than any other machine learning model since the development of machine learning techniques, because it performs generalization at an astonishingly fast speed, needless of mathematically predetermined internal knowledge.

ELM uses datasets in two forms; i.e., training datasets and testing datasets. First of all, ELM model is developed using a training dataset and then verified using a testing dataset. The training and testing datasets have been normalized before using ELM. An enormously fast cognizing algorithm for SLFNs having N' cryptic neurons can be proposed using ELM, where N' ≤ N, considering that N is the number of training samples.

SLFN Approximation Problem

For N distinct random samples (x_i, t_i), where $x_i = [x_{i1}, x_{i2}, x_{i3}, \ldots\ldots, x_{in}]^T \in R^n$

and $t_i = [t_{i1}, t_{i2}, t_{i3}, \ldots\ldots\ldots, t_{im}]^T \in R^m$,

standard SLFNs with N' hidden neurons and activation function g(x) are mathematically modelled as in Equation (5).

$$\sum_{i=1}^{N'} \beta_i g(w_i.\ x_j + b_i) = O_j,\ j = 1, 2, \ldots\ldots, \mathrm{N} \quad (5)$$

where

$w_i = [w_{i1}, w_{i2}, w_{i3}, \ldots\ldots\ldots, w_{in}]^T$ is the weight vector which connects the i^{th} hidden neuron and the input neurons, while the weight vector which connects the i^{th} hidden neuron and the output neurons is $\beta_i = [\beta_{i1}, \beta_{i2}, \beta_{i3}, \ldots\ldots, \beta_{im}]^T$. $w_i * x_j$ denotes the inner product of w_i and x_j.

These N samples can be approximated using standard SLFNs with N' hidden neurons with the activated function g(x),

$$\sum_{j=1}^{N} \| O_j - t_j \| = 0 \quad (6)$$

i.e., there exist β_i, w_i and b_i, such that:

$$\sum_{i=1}^{N'} \beta_i g(w_i.\ x_j + b_i) = O_j,\ j = 1, 2, \ldots\ldots., N \quad (7)$$

The above equations can compactly be written as:

$$H\beta = T \quad (8)$$

where,

$$H\left(w_1,\ \ldots\ldots,\ w_{N'},\ b_1,\ \ldots\ldots,\ b_{N'},\ x_1,\ \ldots\ldots,\ x_N\right) = \begin{bmatrix} g\left(w_1 * x_1 + b_1\right) & \ldots & g\left(w_{N'} * x_1 + b_{N'}\right) \\ \vdots & \ldots & \vdots \\ g\left(w_1 * x_N + b_1\right) & \ldots & g\left(w_{N'} * x_N + b_{N'}\right) \end{bmatrix}_{N*N'} \tag{9}$$

$$\beta = \begin{bmatrix} \beta_1^T \\ \vdots \\ \beta_{N'}^T \end{bmatrix}_{N'*m} \text{ and } T = \begin{bmatrix} t_1^T \\ \vdots \\ t_N^T \end{bmatrix}_{N*m} \tag{10}$$

The i^{th} hidden neuron's output vector is the i^{th} column of H with respect to inputs. x_1, x_2,…… x_n. Interested readers can find more details in Shah et al. (2014).

MARS

MARS, developed by Friedman, is used for developing relations among a group of predictors and subjected variables. MARS uses the strategy of divide and conquer, partitioning training data groups in distinct domains, where every domain gets its own regression string. MARS is dependent on collection and analysis of data procurement.

Generally, if B is the basis function and P stands for the predictor variables, then the predictor of MARS model can be represented using Equation (11).

$$y = \beta_o + \sum_{(j=1)}^{P} \sum_{(b=1)}^{B} [\beta_{jb}(+)Max(0, x_j - H_{bj}) + \beta_{jb}(-)Max(0, H_{bj} - x_j)] \tag{11}$$

If β coefficients of univariate basis functions $Max(0,\ x - H)$ and $Max(0, H - x)$ are 0, they need not to be present.

In MARS algorithm, first of all, from the initial constant basis function, a leading stepwise quest takes place for the basis function. Splitting minimizes "lack of fit" criteria chosen from all possible splits. The process repeats as long as the model clauses the values of certain maximum numbers of pre-decided basis functions (LeBlanc and Tibshirani, 1994). Interested readers can find more information in Yuvaraj et al. (2013).

METHODOLOGY

Dataset and Model Development

In this paper, the generation of data has been carried out according to the database of Zhou et al. (2017). The data contains information on coefficient of cohesion (c; kPa), angle of internal friction (φ; °) and residual tensile strength (σ_t; kPa). A total number of 80 geotechnical datasets have been used in this study to predict the reliability of rock slope. Each of the datasets has been divided into two categories while developing the model. The division of data depends on the problem and on the total number of available datasets. In this study, 70% (i.e., 56) datasets have been adopted for training the model and the remaining 30% (i.e., 24) for testing the model. Prior to using the dataset, it has been normalized using Equation (12).

$$X_{normalized} = \frac{X - X_{\min}}{X_{\max} - X_{\min}} \tag{12}$$

where $X_{normalized}$ is the normalized value, X_{min} is the minimum value from all the events, X_{max} is the maximum value from all the events and X is the particular value of that parameter.

Cubist model has been developed using R script, while ELM and MARS have been developed using MATLAB. Models drawn have a structure of input matrix (x) defined by x = coefficient of cohesion, angle of internal friction and residual tensile strength, while the factor of safety is considered as the target variable (y). All the machine models have used trial and error basis to optimize their prediction.

A graph representing 80 datasets (each of σ_t (kPa), c (kPa), ϕ° and F_s) has been drawn and is shown in Figure 1.

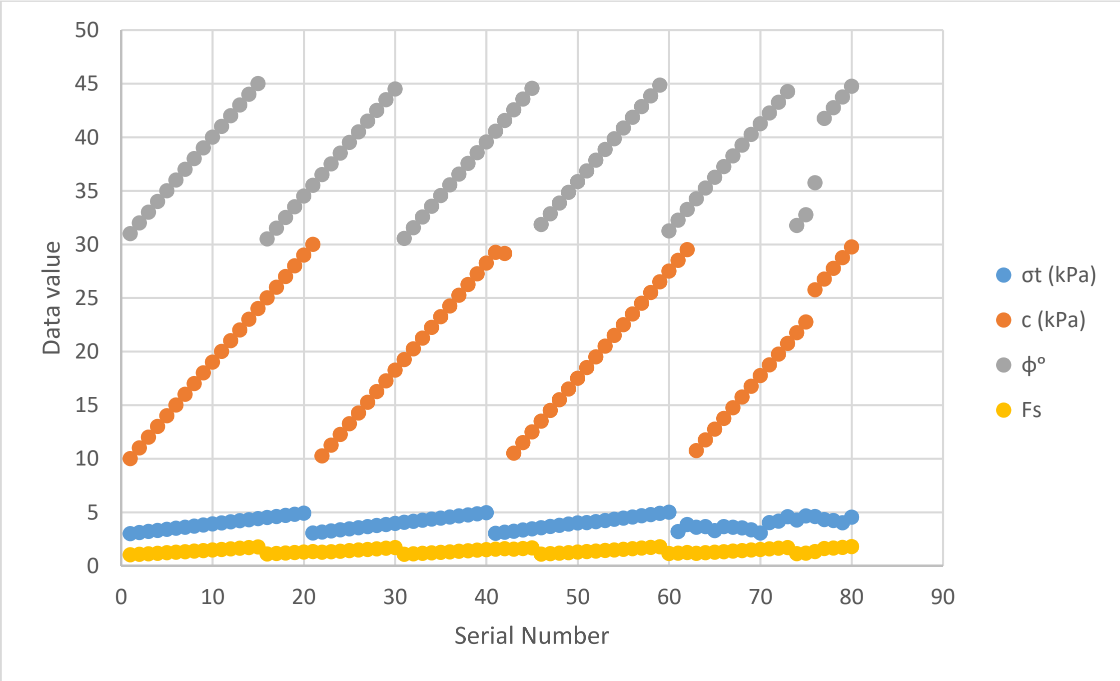

Figure (1): Graph representing datasets of σ_t (kPa), c (kPa), ϕ^o and F_s

Performance Measures

Regression calculates the strength of relationship between different predictors and predictand variables. The fitness and adequacy of the model are justified using various statistical approaches, e.g., weighted mean absolute percentage error (WMAPE); Nash-Sutcliffe efficiency (NS) (Nash and Sutcliffe, 1970); root mean square error (RMSE); variance account factor (VAF); coefficient of determination (R^2); adjusted determination coefficient (Adj. R^2); performance index (PI); bias factor (Armstrong and Collopy, 1992; Wang et al., 2013); root mean square error to observation's standard deviation ratio (RSR); normalized mean bias error (NMBE); mean absolute percentage error (MAPE); mean absolute error (MAE); mean bias error (MBE); sample testing of observed *vs.* predicted value was performed by Legates & McCabe's Index (LMI) (Legates and McCabe, 2013; Legates and McCabe, 1999); relative percent difference (RPD); Willmott's index of agreement (WI) (Willmott, 1984); expanded uncertainty (U95); t-statistic (Stone 1993). While importing data, observed values are mentioned as d_i, whereas predicted values are mentioned as y_i. SD is the standard deviation, N is the number of datasets, p is the number of variables, n is the number of event inputs and d_{mean} is the average of observed values.

1. Weighted mean absolute percentage error (WMAPE) can be calculated using Equation (13).

$$WMAPE = \frac{\sum_{i=1}^{n} \left| \frac{d_i - y_i}{d_i} \right| \times d_i}{\sum_{i=1}^{n} d_i} \tag{13}$$

2. Nash-Sutcliffe efficiency (NS) is the ratio of residual error variance to the measured variance in observed data (Nash and Sutcliffe, 1970) and can be represented using Equation (14).

$$NS = 1 - \frac{\sum_{i=1}^{n} (d_i - y_i)^2}{\sum_{i=1}^{n} (d_i - d_{mean})^2} \tag{14}$$

3. Root mean square error (RMSE) can be calculated as shown in Equation (15).

$$RMSE = \sqrt{\frac{1}{N}\sum_{i=1}^{n}(d_i - y_i)^2} \tag{15}$$

4. Variance account factor can be obtained using Equation (16).

$$VAF = (1 - \frac{\mathrm{var}(d_i - y_i)}{\mathrm{var}(d_i)}) \times 100 \tag{16}$$

5. Coefficient of determination (R^2) value can be obtained using Equation (17).

$$R^2 = \frac{\sum_{i=1}^{n}(d_i - d_{mean})^2 - \sum_{i=1}^{n}(d_i - y_i)^2}{\sum_{i=1}^{n}(d_i - d_{mean})^2} \tag{17}$$

6. Adjusted determination coefficient (Adj. R^2) can be calculated using Equation (18).

$$AdjR^2 = 1 - \frac{(n-1)}{(n-p-1)}(1 - R^2) \tag{18}$$

7. The values of performance index (PI) and the bias factor (Kung et al., 2007; Prasomphan and Machine, 2013) are calculated using Equations (19) and (20).

$$PI = adj.R^2 + 0.01VAF - RMSE \tag{19}$$

$$\text{Bias Factor} = \frac{1}{\mathrm{N}}\sum_{i=1}^{n}\frac{y_i}{d_i} \tag{20}$$

8. RSR includes the benefits of both error index statistics and normalization factor (Moriasi et al., 2007). The most favorable value of RSR is zero. RSR can be calculated using Equation (21).

$$RSR = \frac{RMSE}{\sqrt{\frac{1}{N}\sum_{i=1}^{n}(d_i - d_{mean})^2}} \tag{21}$$

9. NMBE calculates the model strength to forecast values away from mean value (Srinivasulu and Jain, 2006). A positive NMBE represents an over-predicted and a negative NMBE represents an under- predicted model. NMBE is given by Equation (22).

$$NMBE(\%) = \frac{\frac{1}{N}\sum_{i=1}^{n}(y_i - d_i)}{\frac{1}{N}\sum_{i=1}^{n}d_i} \times 100 \tag{22}$$

10. Mean absolute percentage error (MAPE) relates residual error of each event with the observed value (Armstrong and Collopy, 1992). It is a dimensionless quantity and a lower value of MAPE represents superior performance of the model and *vice versa*. MAPE is obtained using Equation (23).

$$MAPE = \frac{1}{N}\sum_{i=1}^{n}\left|\frac{d_i - y_i}{d_i}\right| \times 100 \tag{23}$$

11. Relative percent difference (RPD), suggested by Viscarra Rossel, is used to evaluate the efficiency of the model (Viscarra Rossel, McGlynn and McBratney, 2006). RPD value can be obtained using Equation (24).

$$RPD = \frac{SD}{RMSE} \tag{24}$$

12. Willmott's Index of agreement (WI) value ranges between 0 and 1 (Willmott, 1981, 1982, 1984). The value of 0 represents no match at all, while the value of 1 indicates a perfect match. WI can be calculated using Equation (25).

$$WI = 1 - \left[\frac{\sum_{i=1}^{N} (d_i - y_i)^2}{\sum_{i=1}^{N} \left(| y_i - d_{mean} | + | d_i - d_{mean} | \right)^2} \right], \quad (25)$$

$0 < WI \le 1$

13. Mean absolute error (MAE) can be obtained using Equation (26).

$$MAE = \frac{1}{N} \sum_{i=1}^{n} \left| (y_i - d_i) \right| \quad (26)$$

14. Mean bias error (MBE) can be obtained using Equation (27).

$$MBE = \frac{1}{N} \sum_{i=1}^{n} (y_i - d_i) \quad (27)$$

15. Legate and McCabe's Index, LMI, varies from 0 to 1. For better model fit, the value of LMI should be closer to 1 (Legates and Davis, 1997; Legates and McCabe, 2013; Legates and McCabe, 1999). LMI can be calculated using Equation (28).

$$LMI = 1 - \left[\frac{\sum_{i=1}^{N} | d_i - y_i |}{\sum_{i=1}^{N} | d_i - d_{mean} |} \right], \quad 0 < LMI \le 1 \quad (28)$$

16. U_{95} compares the actual deviation amidst calculated value and measured value and thus examines short-term performance of the model. The formula in Equation (29) provides uncertainty at 95% confidence level. 1.96 is the coverage factor subsequent to confidence level. Expanded uncertainty (U_{95}) (Behar, Khellaf and Mohammedi, 2015; Gueymard, 2014) can be formulated as:

$$U_{95} = 1.96 (SD^2 + RMSE^2)^{1/2} \quad (29)$$

17. t-statistic determines whether the prediction of the model at a particular confidence level is statistically significant or not. It is one of the most widely accepted parameters. t-statistic compares sample mean(s) to the null hypothesis. Smaller values of t-statistic indicate superior performance of the model. The value of zero accepts the null hypothesis, while an increase in the absolute value of t-statistic corresponds to an increase in the sample data and null hypothesis. t-statistic (Stone, 1993) can be given by Equation (30).

$$t\text{-stat} = \sqrt{\frac{(N-1) MBE^2}{RMSE^2 - MBE^2}} \quad (30)$$

RESULTS AND DISCUSSION

In this research, three soft computing techniques (cubist model tree, ELM and MARS) were used for the assessment of rock slope reliability analysis. A comparison has been carried out between them considering different statistical indicators, like variance account factor, RMSE, MAPE, R^2, relative percentage difference (RPD) (Viscarra Rossel et al., 2006), receiver operating characteristic (ROC), …etc. All the three models showed significant results in terms of all fitness parameters. Coefficient of determination (R^2) values for all the models were close to 1 in both training and testing cases. Adjusted determination coefficient (Adj. R^2) values were almost equal to 1 in both training and testing cases. A value of NS closer to one indicates the accuracy of the model. The value of RSR is good for all the models. All the models gave values closer to zero for mean absolute error (MAE) in both training and testing cases, which shows the excellency of the models used. Values of MBE were almost zero in all the training and testing outputs using different models taken into consideration. All models showed good results of LMI as well. Values of different statistical parameters are shown in Table 1.

Table 1. Statistical parameters of cubist, ELM and MARS models

Parameters	Cubist		ELM		MARS	
	Training	Testing	Training	Testing	Training	Testing
NS	0.999	0.999	0.999	0.998	0.999	0.999
RMSE	0.0045	0.006	0.006	0.009	0.002	0.003
VAF	99.955	99.89	99.91	99.778	99.990	99.981
R^2	0.999	0.999	0.999	0.998	0.999	0.999
Adj R^2	0.999	0.998	0.999	0.997	0.999	0.999
PI	1.994	1.99	1.991	1.986	1.998	1.997
Bias Factor	0.999	0.999	1	1	1	1
RSR	0.021	0.033	0.029	0.049	0.009	0.014
NMBE	-0.041	-0.013	-0.0005	0.151	0.009	0.026
MAPE	0.244	0.316	0.387	0.494	0.124	0.142
RPD	46.932	30.288	33.522	20.608	101.856	72.128
WI	0.999	0.999	0.999	0.999	0.999	0.999
MAE	0.003	0.004	0.005	0.007	0.002	0.002
MBE	-0.0006	-0.0002	0	0.002	0.0001	0.0004
LMI	0.98	0.97	0.97	0.96	0.99	0.99
U_{95}	0.42	0.36	0.42	0.36	0.42	0.36
t-stat	0.93	0.148	0.009	1.178	0.456	0.696
β	1.774	2.162	1.772	2.163	1.774	2.186

A graph between actual and predicted values of factor of safety of training and testing cases for cubist model has been drawn, as shown in Figure 2.

All the values of training and testing data are close to the predicted line, which indicates a high prediction ability.

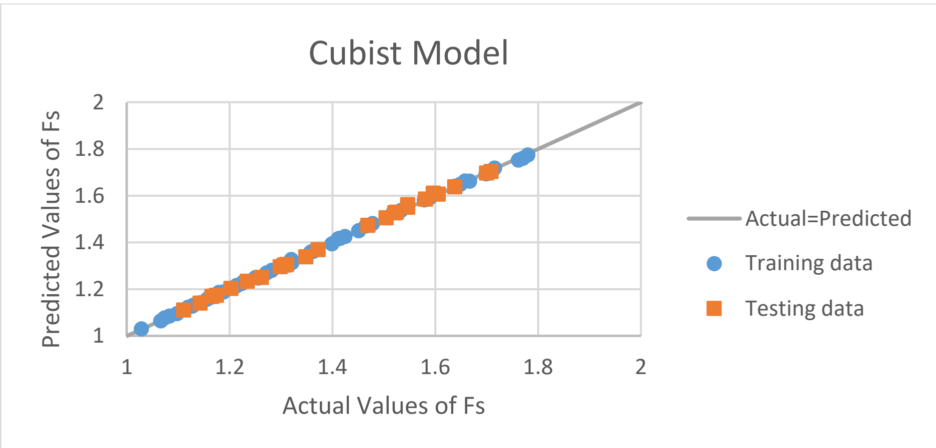

Figure (2): Actual *vs.* predicted values of training and testing data using cubist model

A graph between actual and predicted values of factor of safety of training and testing cases for ELM model has been drawn, as illustrated in Figure 3.

All the values of training and testing data are close to the predicted line, which shows that the model prediction ability is high.

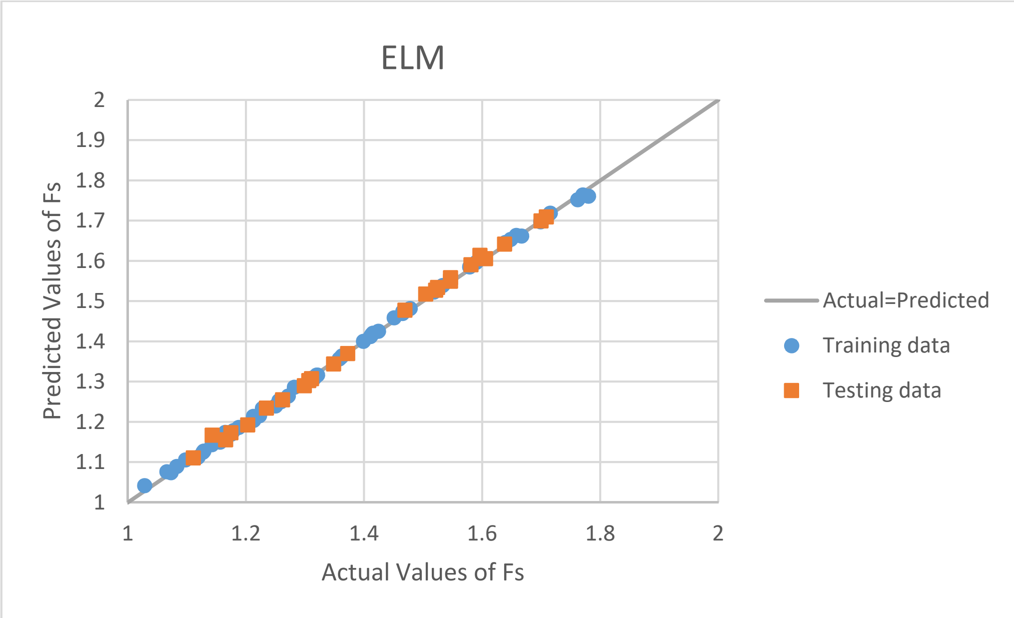

Figure (3): Actual *vs.* predicted values of training and testing data using ELM model

A graph between actual and predicted values of factor of safety of training and testing cases for MARS model has been drawn, as shown in Figure 4.

All the values of training and testing data are close to the predicted line, which shows that the model prediction ability is high.

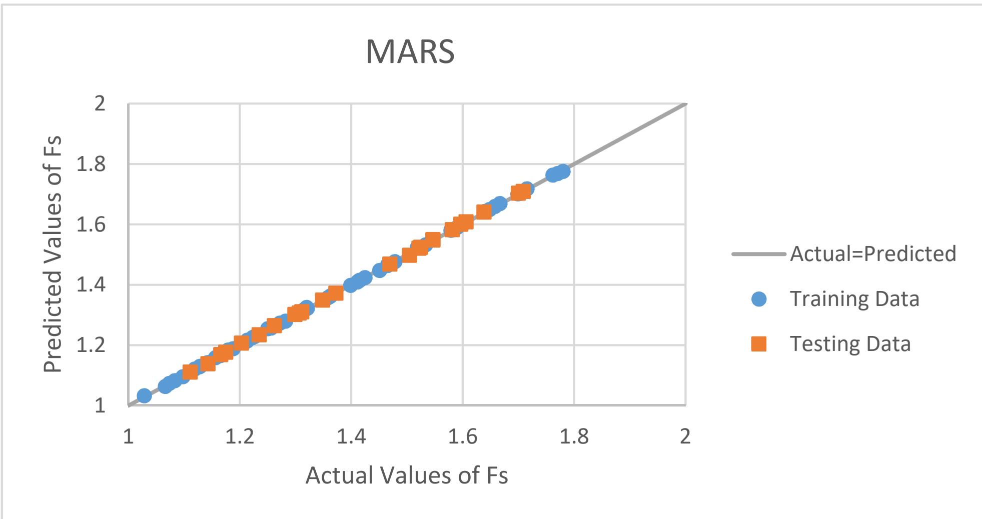

Figure (4): Actual *vs.* predicted values of training and testing data using MARS model

Taylor diagram provides a path to plot three different statistics on a 2D graph indicating the closeness of pattern to the observations (Taylor, 2001). For each model, three statistics as correlation coefficients are related to the azimuthal angle, represented by black dotted contours generating from the origin, root mean square error, represented by red contours and the third one is the standard deviation of the stipulated pattern, represented by proportioning through radial distance from the origin. Taylor diagram makes it convenient to differentiate between different models and to distinguish which model is the best compared to the other models.

Taylor diagram for training cases of different models has been plotted and the outcome is as shown in Figure 5.

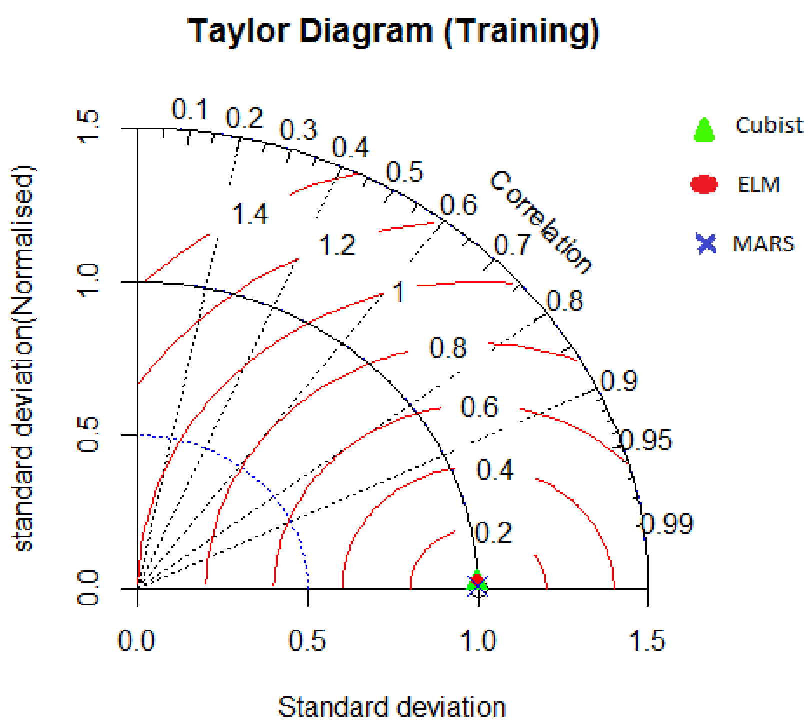

Figure (5): Taylor diagram (training)

From the curve in Figure 5, it is clear that the correlation coefficient of each model is greater than 0.99, the root mean square error value is close to zero and the standard deviation of each stipulated model is 1. All the models are giving values close to each other and accumulating to make a point.

Taylor diagram for testing cases of different models has been plotted and the outcome is as shown in Figure 6.

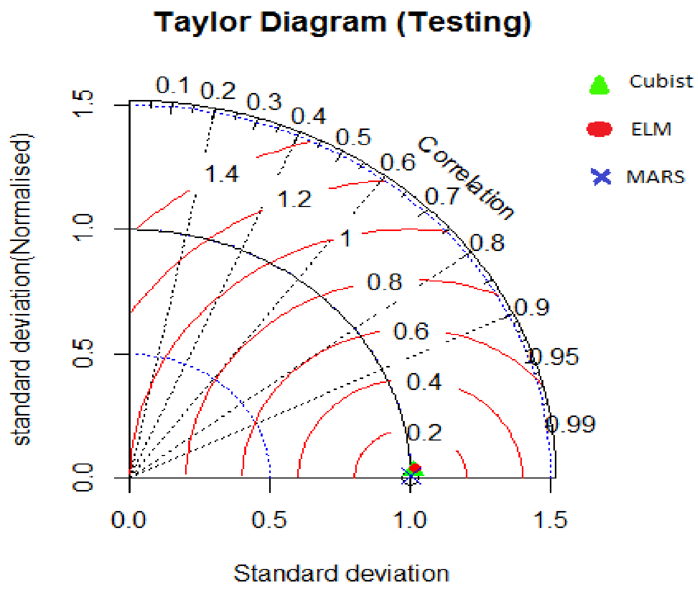

Figure (6): Taylor diagram (testing)

From Figure 6, it can be seen that all the models give values close to each other; hence, also in the case of testing of dataset, values from these models accumulate to make a point.

ROC curve gives an idea about the performance of the models used. The area covered on x-axis represents the area under curve of the model. Higher area under curve represents a good performance of the model. Different curves have been drawn using training and testing values of the models used and the outcome is as shown in Figure 7.

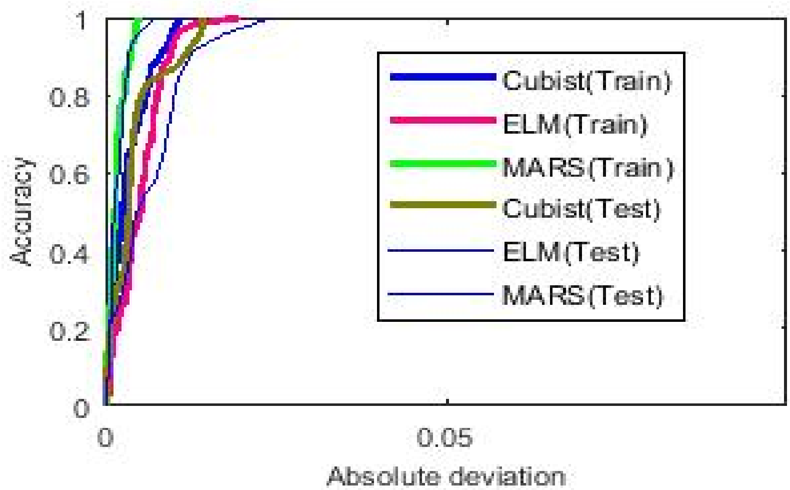

Figure (7): ROC curve (training and testing)

From the ROC curve (Figure 7), we can conclude that MARS model in both training and testing is showing the best performance among the three models.

Reliability index (β) of observed data for training is 1.7713 and for testing is 2.1889.

A comparison between reliability values of training cases has been carried out, as shown in Figure 8.

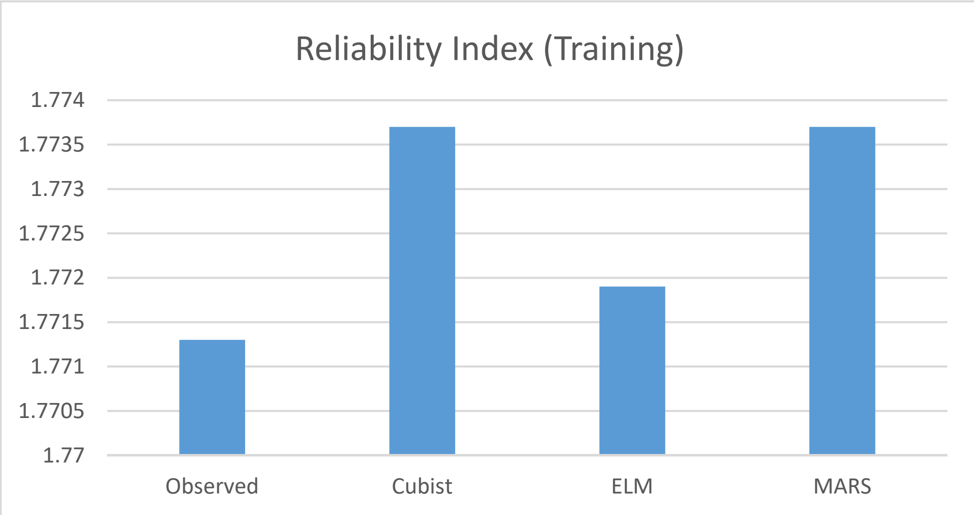

Figure (8): Reliability index values of training case

A comparison between reliability values of testing cases has been carried out as shown in Figure 9.

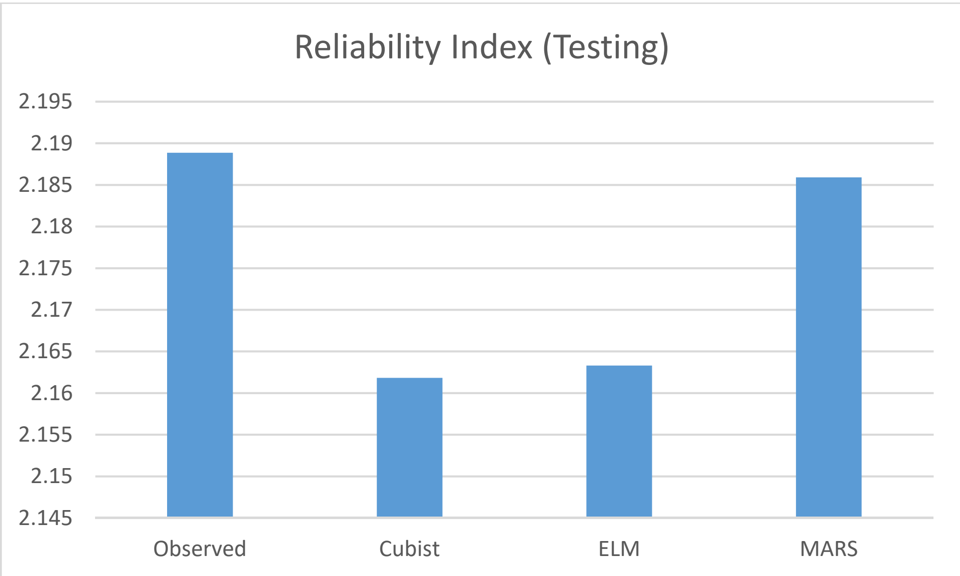

Figure (9): Reliability index values of testing case

CONCLUSIONS

In this article, the verification of usefulness of three models of advanced soft computing (MARS, ELM and cubist) has been carried out for calculating the reliability of rock slope and evaluating the reliability obtained. Since all the methods used are data-specific, hence based on their efficiency on the utilized data, different outputs were obtained. Here, for the study of slope failure and geological condition, a total of 80 cases were used. Soft computing parameters, like R^2, Adj.R^2, MAE, MBE, AUC, … etc., were used for assessing the performance of soft computing models. From the abstracted results (from ROC curves), the largest value of area under curve (AUC) was obtained for MARS model, followed by cubist model and then by ELM model. All these models give prominent results to use them for reliability analysis of rock slope, but if we have to choose one from these models, then MARS model comes out to be the best. Training and testing data accumulated up while graphing Taylor and ROC curves. This article gives an idea of using computational methods and models in forecasting and analyzing the reliability of rock slope and can also be used in the field of geotechnical engineering while calculating other parameters.

REFERENCES

Armstrong, J. Scott, and Fred Collopy. (1992). “Error measures for generalizing about forecasting methods: empirical comparisons”. International Journal of Forecasting, 8 (1), 69-80.

Baecher, G. B., and J. T. Christian. (2003). “Reliability and statistics in geotechnical engineering”. Technometrics, 618.

Behar, Omar, Abdallah Khellaf, and Kamal Mohammedi. (2015). “Comparison of solar radiation models and their validation under Algerian climate: the case of direct irradiance”. Energy Conversion and Management, 98, 236-251.

Breiman, Leo. (2017). “Classification and regression trees”.

Duzgun, H.S.B., Yucemen, M.S., and Celal Karpuz. (2003). “A Methodology for reliability-based design of rock slopes”. Rock Mechanics and Rock Engineering, 36 (2), 95-120.

Ganji, A., and L. Jowkarshorijeh. (2012). “Advance first-order second-moment (AFOSM) method for single reservoir operation reliability analysis: a case study”. Stochastic Environmental Research and Risk Assessment, 26 (1), 33-42.

Ge, Haiyu, Jinsong Tu, and Fengyan Qin. (2011). “Analysis of slope stability with first-order second-moment method”. International Journal of Digital Content Technology and Applications, 5 (12), 445-451.

Gravanis, Elias, Lysandros Pantelidis, and Griffiths, D.V. (2014). “An analytical solution in probabilistic rock slope stability assessment based on random fields”. International Journal of Rock Mechanics and Mining Sciences, 71, 19-24.

Gueymard, C.A. (2014). “A review of validation methodologies and statistical performance indicators for modeled solar radiation data: towards a better bankability of solar projects”. Renewable and Sustainable Energy Reviews, 39, 1024-1034.

Harr, Edward Milton. (1987). “Reliability-based design in civil engineering”.

Huang, Guang Bin. (2003). “Learning capability and storage capacity of two-hidden-layer feedforward networks”. IEEE Transactions on Neural Networks, 14 (2), 274-281.

Jiang, Shui Hua, Dian Qing Li, Li Min Zhang, and Chuang Bing Zhou. (2014). “Slope reliability analysis considering spatially variable shear strength parameters using a non-intrusive stochastic finite element method”. Engineering Geology, 168, 120-128.

Jimenez-Rodriguez, R., and N. Sitar. (2007). "Rock wedge stability analysis using system reliability methods". Rock Mechanics and Rock Engineering, 40 (4), 419-427.

Khalokakaie, Reza, and Masoud Zare Naghadehi. (2012). "Ranking the rock slope instability potential using the interaction matrix (IM) technique; a case study in Iran". Arabian Journal of Geosciences, 5 (2), 263-273.

Kourosh, M. A., S. Mosrafa, and S. M. Heydari. (2011). "Uncertainty and reliability analysis applied to slope stability: a case study from Sungun copper mine". Geotechnical and Geological Engineering, 29 (4), 581-596.

Kuhn, Max, Steve Weston, Chris Keefer, and Nathan Coulter. (2016). "Cubist models for regression". R Package Vignette, Version 0.0 18.

Kung, Gordon T., C. Hsein Juang, Evan C. Hsiao, and Youssef M. Hashash. (2007). "Simplified model for wall deflection and ground-surface settlement caused by braced excavation in clays". Journal of Geotechnical and Geoenvironmental Engineering, 133 (6), 731-747.

LeBlanc, Michael and Robert Tibshirani. (1994). "Adaptive principal surfaces". Journal of the American Statistical Association, 89 (425), 53-64.

Legates, David R., and Gregory J. McCabe. (2013). "A refined index of model performance: a rejoinder". International Journal of Climatology, 33 (4), 1053-1056.

Legates, David R., and Robert E. Davis. (1997). "The continuing search for an anthropogenic climate change signal: limitations of correlation-based approaches". Geophysical Research Letters, 24 (18), 2319-2322.

Legates, David R., and Gregory J. McCabe. (1999). "Evaluating the use of 'goodness-of-fit' measures in hydrologic and hydroclimatic model validation". Water Resources Research, 35 (1), 233-241.

Li, Ang, Guo Jian Shao, Pei Rong Du, Sheng Yong Ding, and Jing Bo Su. (2015). "Numerical studies on stratified rock failure based on digital image processing technique at mesoscale". Computers, Materials and Continua, 45, 17-38.

Li, Dian Qing, Xiao Song Tang, and Kok Kwang Phoon. (2015). "Bootstrap method for characterizing the effect of uncertainty in shear strength parameters on slope reliability". Reliability Engineering and System Safety, 140, 99-106.

Li, Liang, Yu Wang, and Zijun Cao. (2014). "Probabilistic slope stability analysis by risk aggregation". Engineering Geology, 176, 57-65.

Li, Shaojun, Hong-Bo Zhao, and Zhongliang Ru. (2013). "Slope reliability analysis by updated support vector machine and Monte Carlo simulation". Natural Hazards, 65 (1), 707-722.

Liang, Li, and Chu Xue-song. (2012). "The location of critical reliability slip surface in soil slope stability analysis". Procedia-Earth and Planetary Science, 5, 146-149.

Liu, Ya-Ching, and Chao-Shi Chen. (2007). "A new approach for application of rock mass classification on rock slope stability assessment". Engineering Geology, 89 (1-2), 129-143.

Liu, Zaobao, Weiya Xu, and Jianfu Shao. (2012). "Gauss process-based approach for application on landslide displacement analysis and prediction". CMES-Computer Modeling in Engineering and Sciences, 84 (2), 99.

Moriasi, D.N., Arnold, J.G., Van Liew, M.W., Bingner, R.L., Harmel, R.D., and T.L. Veith. (2007). "Model evaluation guidelines for systematic quantification of accuracy in watershed simulations". Transactions of the ASABE, 50 (3), 885-900.

Nash, J.E., and J.V. Sutcliffe. (1970). "River flow forecasting through conceptual models part I: a discussion of principles". Journal of Hydrology, 10 (3), 282-290.

Pariseau, William G., Saurabh Puri, and Steve C. Schmelter. (2008). "A new model for effects of impersistent joint sets on rock slope stability". International Journal of Rock Mechanics and Mining Sciences, 45 (2), 122-131.

Park, Hyuck Jin, Jeong Gi Um, Ik Woo, and Jeong Woo Kim. (2012). "The evaluation of the probability of rock wedge failure using the point estimate method". Environmental Earth Sciences, 65 (1), 353-361.

Park, Hyuck Jin, Jeongi-Gi Um, Ik Woo, and Jeong Woo Kim. (2012). “Application of fuzzy set theory to evaluate the probability of failure in rock slopes”. Engineering Geology, 125, 92-101.

Park, Hyuck Jin, Jung Hyun Lee, Kang Min Kim, and Jeong Gi Um. (2016). “Assessment of rock slope stability using GIS-based probabilistic kinematic analysis”. Engineering Geology, 203, 56-69.

Park, Hyuck Jin, Terry R. West, and Ik Woo. (2005). “Probabilistic analysis of rock slope stability and random properties of discontinuity parameters, Interstate Highway 40, Western North Carolina, USA”. Engineering Geology, 79 (3-4), 230-250.

Pathak, Shubh, and Bjørn Nilsen. (2004). “Probabilistic rock slope stability analysis for Himalayan condition”. Bulletin of Engineering Geology and the Environment, 63 (1), 25-32.

Prasomphan, S., and S. Mase Machine. (2013). “Generating prediction map for geostatistical data based on an adaptive neural network using only nearest neighbors”. International Journal of Machine Learning and Computing, 3 (1), 98.

Quinlan, J. R. (2014). "C4.5: programs for machine learning".

Reale, Cormac, Jianfeng Xue, Zhangming Pan, and Kenneth Gavin. (2015). “Deterministic and probabilistic multi-modal analysis of slope stability”. Computers and Geotechnics, 66, 172-179.

Shah, Vishal Shreyans, Henyl Rakesh Shah, Pijush Samui, and A. Ramachandra Murthy. (2014). “Prediction of fracture parameters of high-strength and ultra-high-strength concrete beams using minimax probability machine regression and extreme learning machine”. Computers, Materials and Continua, 44 (2), 73-84.

Srinivasulu, Sanaga, and Ashu Jain. (2006). “A comparative analysis of training methods for artificial neural network rainfall-runoff models”. Applied Soft Computing Journal, 6 (3), 295-306.

Stone, R. J. (1993). “Improved statistical procedure for the evaluation of solar radiation estimation models”. Solar Energy, 51 (4), 289-291.

Sun, B., S. Zeng, and D. Ding. (2008). “Study and application of reliability analysis method in open-pit rock slope project”. 899-906, in: Geotechnical Engineering for Disaster Mitigation and Rehabilitation.

Tan, Xiao Hui, Meng Fen Shen, Xiao liang Hou, Dan Li, and Na Hu. (2013). “Response surface method of reliability analysis and its application in slope stability analysis”. Geotechnical and Geological Engineering, 31 (4), 1011-1025.

Taylor, Karl E. (2001). “Summarizing multiple aspects of model performance in a single diagram”. Journal of Geophysical Research Atmospheres, 106 (D7), 7183-7192.

Topal, T. (2007). “Discussion of ‘a new approach for application of rock mass classification on rock slope stability assessment’ by Liu and Chen, Engineering Geology, 89, 129-143 (2007)”. Engineering Geology, 3 (95), 99-100.

Viscarra Rossel, R. A., R. N. McGlynn, and A.B. McBratney. (2006). “Determining the composition of mineral-organic mixes using UV-VIS-NIR diffuse reflectance spectroscopy”. Geoderma, 137 (1-2), 70-82.

Wang, Lei, Jin Hung Hwang, C. Hsein Juang, and Sez Atamturktur. (2013). “Reliability-based design of rock slopes: a new perspective on design robustness”. Engineering Geology, 154, 56-63.

Wei, Lun Wei, Hongey Chen, Ching Fang Lee, Wei Kai Huang, Ming Lang Lin, Chung Chi Chi, and Hsi Hung Lin. (2014). “The mechanism of rockfall disaster: a case study from Badouzih, Keelung in northern Taiwan”. Engineering Geology, 183, 116-126.

Willmott, Cort J. (1981). “On the validation of models”. Physical Geography, 2 (2), 184-194.

Willmott, Cort J. (1982). “Some comments on the evaluation of model performance”. Bulletin of the American Meteorological Society, 63 (11), 1309-1313.

Willmott, Cort J. (1984). “On the evaluation of model performance in physical geography”. 443-460, in: Spatial Statistics and Models.

Yang, Zhi-gang, Tong-chun Li, and Miao-lin Dai. (2009). "Reliability analysis method for slope stability based on sample weight". Water Science and Engineering, 2 (3), 78-86.

Youssef, Ahmed M., Biswajeet Pradhan, and Saad G. Al-Harthi. (2015). "Assessment of rock slope stability and structurally controlled failures along Samma Escarpment Road, Asir Region (Saudi Arabia)". Arabian Journal of Geosciences, 8 (9), 6835-6852.

Yuvaraj, P., A. Ramachandra Murthy, Nagesh R. Iyer, Pijush Samui, and S. K. Sekar. (2013). "Multivariate adaptive regression splines model to predict fracture characteristics of high-strength and ultra-high-strength concrete beams". Computers, Materials and Continua, 36 (1), 73-97.

Zhou, Jia-wen, Ming-yuan Jiao, Hui-ge Xing, Xing-guo Yang, and Yu-chuan Yang. (2017). "A reliability analysis method for rock slope controlled by weak structural surface". Geosciences Journal, 21 (3), 453-467.

Zhou, Jia Wen, Wei Ya Xu, Xing Guo Yang, Chong Shi, and Zhao Hui Yang. (2010). "The 28 October 1996 landslide and analysis of the stability of the current Huashiban slope at the Liangjiaren hydropower station, southwest China". Engineering Geology, 114 (1-2), 45-56.